

Analysis of an Intermediate-Mode-Assisted Directional Coupler Using Bloch Theory

Alexander M. Kenis, Ilya Vorobeichik, and Nimrod Moiseyev

Abstract—The exact numerical solution of the intermediate-mode-assisted directional coupler problem is obtained using the Bloch wave approach. The approach is based on a calculation of the Bloch waves and their matching with the ideal modes of a uniform waveguide. The approximate results obtained from the paraxial wave equation and from the three-mode model are compared with the exact ones. It is shown that the paraxial approximation, as well as the three-mode approximation, provide only a qualitatively correct physical picture. Using the Bloch wave approach, however, one obtains quantitatively correct results. It is demonstrated that one can control the exchange of power between two distant identical coupled waveguides using an embedded periodic structure along the z direction. The power exchange control is based on a symmetry of Bloch waves and results from the interaction of the lowest order waveguide modes with the high-order modes.

Index Terms—Directional couplers, numerical analysis, optical waveguides, periodic structures.

I. INTRODUCTION

OPTICAL waveguides with embedded periodic structures are important for many applications in integrated optics and optical communications. They can be used for mode- and power-coupling in optical devices, such as couplers, wavelength filters, light switches, and modulators [1]–[11]. Calculation of the amplitudes of forward- and backward-propagating waves is the most important part in performance simulations of these devices. The common approach to the solution of this problem is coupled-mode theory (CMT) (see, e.g., [1], [2], [12]–[15]), which is based on the expansion of the solution of the wave equation in terms of ideal or local modes of a uniform optical waveguide. The coupled differential equations for the coefficients of these modes are then solved by a numerical propagation. CMT is an efficient method that can be applied to both periodic and nonperiodic gratings. For periodic gratings, one can also use approximate closed-form solutions for the coupled-mode equations [1]. However, the implementation of the analytical expressions of CMT becomes problematic as the number of coupled modes increases. The numerical solution of the coupled-mode equations by step-by-step propagation also becomes difficult for periodic structures that consist of

a large number of grating periods. In the case of long-range periodic inhomogeneities of the refractive index, an alternative Bloch wave approach (see, e.g., [16]–[19]) can be used. The Bloch wave approach involves first obtaining the full set of normal modes that are permitted in the periodic medium, and then identifying those that are excited by matching to the incident-plane-waves along the boundaries. Although this approach can only be applied to uniform (periodic) gratings, the Bloch approach can clarify features of propagation in periodic media that are not immediately clear and sometimes difficult to interpret when the coupled-wave approach is adopted [16]. This is true, particularly, in cases where the Bloch waves are significantly different from the modes of the uniform waveguide. Then, the number of ideal (or local) modes needed for the description of propagation in the periodic medium may be quite large, thus making both the numerical computation and physical interpretation of the results using CMT more difficult.

In this paper, we apply the Bloch wave approach to the intermediate-mode-assisted optical coupler formerly studied in the framework of the paraxial approximation [20]. It was demonstrated that the embedded periodic structure can be used to enhance or suppress the directional coupling by many orders of magnitude. The control of the directional coupling was explained by studying the dependence of the eigenphases of forward-propagating modes of the periodic structure on the grating parameters. The enhancement and suppression of the directional coupling were shown to be due to the avoided or exact crossing between the eigenphases. We use the Bloch wave approach to calculate the wavevectors of both forward- and backward-propagating Bloch waves and to compare the numerically exact results with the approximate results obtained in the framework of the paraxial approximation. The amplitudes of the reflected and transmitted waves are calculated as well.

In Section II, the Bloch wave technique is described. In Section III, the method is applied to the intermediate-mode-assisted optical coupler. In Section IV, we conclude.

II. BLOCH WAVES AND MATCHING

We consider planar optical waveguide structures, where the transverse Cartesian component of the electric field $E_y(x, z)$ satisfies the scalar wave equation of the form

$$\left[\nabla_{x,z}^2 + \frac{\omega^2}{c^2} n^2(x, z) \right] E_y(x, z) = 0 \quad (1)$$

where $n(x, z)$ is the index of refraction distribution and $\omega/c = 2\pi/\lambda = k$ is the wavevector in free space. When other Cartesian components of the electric field are considered or when

Manuscript received October 6, 1999; revised January 10, 2000.

A. M. Kenis is with the Department of Physics, Technion—Israel Institute of Technology, Haifa 32000, Israel.

I. Vorobeichik is with the Department of Chemistry and the Department of Electrical Engineering, Technion—Israel Institute of Technology, Haifa 32000, Israel.

N. Moiseyev is with the Department of Chemistry and Minerva Center for Non-Linear Physics of Complex Systems, Technion—Israel Institute of Technology, Haifa 32000, Israel.

Publisher Item Identifier S 0018-9197(00)03537-5.

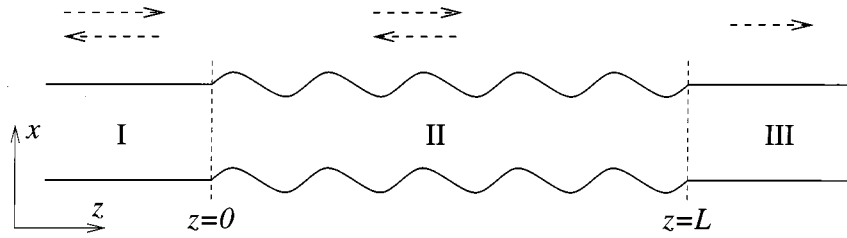


Fig. 1. A schematic representation of the refractive index distribution. In region I: the refractive index is z -independent ($n = n(x)$), a right arrow stands for the incoming wave, and a left arrow for the reflected waves. In region II: the refractive index is periodic ($n = n(x, z) = n(x, z + \Lambda)$) and a right/left arrow stands for the forward-/backward-propagating Bloch waves. In region III: the refractive index is z -independent and a right arrow stands for the transmitted waves.

a three-dimensional (3-D) waveguide is studied, then, in general, polarization effects should be taken into account. For simplicity, we studied the scalar wave equation (1), but the generalization of the method for the vector wave equation is straightforward. Moreover, the scalar wave approximation can be used for weakly guiding waveguides with moderate gratings (i.e., grating periods which are much larger than the optical wavelength and small grating amplitudes) in which the polarization effects can be neglected.

The index of refraction distribution $n(x, z)$ is schematically shown in Fig. 1.

Formally,

$$n(x, z) = \begin{cases} n(x) & \text{when } z < 0 \\ n(x, z) = n(x, z + \Lambda) & \text{when } 0 \leq z \leq L \\ n(x) & \text{when } z > L \end{cases} \quad (2)$$

where Λ is the period of the refractive index variations and L is the length of the periodic structure. Since the refractive index is z -independent asymptotically (i.e., for $z < 0$ and $z > L$), one can easily calculate the solutions of the wave equation in the asymptotic regions. These solutions are given by

$$\Psi_j^{\pm(0)} = e^{\pm i\beta_j z} \Phi_j^{(0)}(x), \quad (3)$$

where $\Phi_j^{(0)}(x)$ satisfies

$$\left[\nabla_x^2 + \frac{\omega^2}{c^2} n^2(x) \right] \Phi_j^{(0)}(x) = \beta_j^2 \Phi_j^{(0)}(x) \quad (4)$$

and we have replaced $E_y(x, z)$ in (1) for $\Psi(x, z)$. We assume that an optical wave arrives from $z = -\infty$ such that the solution in region I ($z < 0$) is given by the linear combination of the incoming and reflected waves

$$\Psi_{\text{I}} = \sum_j C_j^{(0)} \Psi_j^{+(0)} + \sum_j R_j \Psi_j^{- (0)} \quad (5)$$

where $C_j^{(0)}$ is the coefficient of ideal mode $\Phi_j^{(0)}$ contributing to the incoming wave and R_j is the amplitude of the reflected wave $\Psi_j^{- (0)}$. The optical wave in region III ($z > L$) is given by the linear combination of transmitted waves

$$\Psi_{\text{III}} = \sum_j T_j \Psi_j^{+(0)} \quad (6)$$

where T_j is the amplitude of the transmitted wave $\Psi_j^{+(0)}$. If one were to follow the CMT scheme [12], one would expand the solution in region II in terms of ideal modes $\Psi_j^{(0)}$ and solve the set

of the coupled differential equations for the expansion coefficients by a numerical propagation. However, for periodic structures that consist of many periods, one can use the refractive index periodicity to avoid a long-distance propagation. Since, for $0 \leq z \leq L$, the refractive index is periodic, the solution of the wave equation in this region of space is given in terms of Bloch waves. Therefore, in this region, one can apply the Bloch theorem [21] to analytically “propagate” the solution from $z = 0$ to $z = L$.

According to the Bloch theorem [21], the solution of (1) for a periodic refractive index

$$n(x, z + \Lambda) = n(x, z) \quad (7)$$

is given by

$$\Psi_k(x, z) = e^{ikz} \Phi_k(x, z) \quad (8)$$

where $\Phi_k(x, z)$ is a periodic Bloch function such that

$$\Phi_k(x, z) = \Phi_k(x, z + \Lambda) \quad (9)$$

and k is the Bloch wavevector that varies continuously in the first Brillouin zone of the reciprocal lattice, i.e., from $-\pi/\Lambda$ to π/Λ . Substitution of (8) into (1) leads to

$$\left[\left(\frac{\partial}{\partial z} + ik \right)^2 + \frac{\partial^2}{\partial x^2} + \frac{\omega^2}{c^2} n^2(x, z) \right] \Phi_k(x, z) = 0. \quad (10)$$

After (10) is solved and the Bloch solutions in region II are obtained, the amplitudes of the reflected and transmitted waves can be calculated by matching the asymptotic and Bloch solutions (and their derivatives) at the region boundaries, i.e., $z = 0$ and $z = L$. However, the main advantage of the Bloch wave approach is the insight into the waveguide properties gained by understanding of the dependence of the Bloch wavevectors on the parameters of the grating and on the wavelength.

Unfortunately, (10) is not an eigenvalue problem and cannot be solved by straightforward diagonalization methods. To calculate the Bloch solutions, one can first solve

$$\left[\left(\frac{\partial}{\partial z} + ik \right)^2 + \frac{\partial^2}{\partial x^2} + \frac{\omega^2}{c^2} n^2(x, z) \right] \Phi_k = \xi_k \Phi_k \quad (11)$$

and then find the Bloch wavevectors as the roots of

$$\xi_{k_i} = 0, \quad i = 1, 2, \dots \quad (12)$$

One may adopt a different strategy for the solution of (10) by rewriting it in the following form:

$$\frac{1}{n} \left[- \left(\frac{\partial}{\partial z} + ik \right)^2 - \frac{\partial^2}{\partial x^2} \right] \frac{1}{n} \tilde{\Phi}_k = \frac{\omega^2}{c^2} \tilde{\Phi}_k \quad (13)$$

where

$$\tilde{\Phi}_k(x, z) = n(x, z) \Phi_k(x, z). \quad (14)$$

Unlike (10), (13) is a typical eigenvalue problem and, therefore, this strategy is preferable when one is interested in calculating the dispersion relation $\omega(k)$ of a periodic structure (as it is done in photonic bandgap studies [22]). This approach, however, has a disadvantage that is due to the fact that the operator on the left-hand side of (13) is not separable and couples different directions even if n is separable. This makes the use of ideal modes as a basis set impractical. Therefore, when a CW case is studied and a relatively small number of ideal modes can be used to describe the optical wave, then (10) is usually a better way to calculate the Bloch solutions.

The solution of (1) for $0 \leq z \leq L$ can be written as

$$\Psi_{\text{II}} = \sum_j C_j^+ \Psi_j^+(x, z) + C_j^- \Psi_j^-(x, z) \quad (15)$$

where

$$\Psi_j^\pm(x, z) = e^{\pm ik_j z} \Phi_j^\pm(x, z) \quad (16)$$

and $\Phi_j^+(x, z)$ and $\Phi_j^-(x, z)$ are the Bloch functions that correspond to forward- and backward-traveling waves, respectively. Since the operator on the left-hand side of both (10) and (13) is Hermitian, then

$$\Phi_j^+ = (\Phi_j^-)^*. \quad (17)$$

C_j^\pm are coefficients of different Bloch waves $\Phi_j^\pm(x, z)$ that contribute to the solution of the wave equation in region II.

In order to calculate the reflection and transmission amplitudes for the incoming wave of interest, we represent the solution of the wave equation in each of the three regions in a basis set of the asymptotic ideal modes ($\Phi_j^{(0)}(x)$, $j = 1, 2, \dots, N$) [see (4)]. Then one can write the solution in each region in a vector form, in which a j th component of a vector represents the coefficient of $\Phi_j^{(0)}$ in the expansion of the solution. In this form, the asymptotic solution and its derivative in region I at $z = 0$ are given by

$$\vec{\Psi}_1(0) = \vec{\Psi}^{(i)}(0) + \mathbf{E}_-(0) \vec{R} \quad (18)$$

$$\vec{\Psi}'_1(0) = \vec{\Psi}^{(i)'}(0) + \mathbf{E}'_-(0) \vec{R} \quad (19)$$

where $\Psi^{(i)}$ is the incoming wave introduced into (5) as

$$\Psi^{(i)} = \sum_j C_j^{(0)} \Psi_j^{+(0)} \quad (20)$$

(bold face letters and arrows denote matrices and vectors, respectively, and a prime denotes the first derivative with respect to z). Thus,

$$\vec{\Psi}^{(i)}(0) = (C_1^{(0)}, C_2^{(0)}, \dots, C_N^{(0)}) \quad (21)$$

$$\vec{\Psi}^{(i)'}(0) = i (\beta_1 C_1^{(0)}, \beta_2 C_2^{(0)}, \dots, \beta_N C_N^{(0)}) \quad (22)$$

$$\vec{R} = (R_1, R_2, \dots, R_N). \quad (23)$$

$\mathbf{E}'_-(0)$ is a diagonal matrix with $[\mathbf{E}'_-(0)]_{j,j} = -i\beta_j$, and $\mathbf{E}_-(0)$ is a unit matrix.

Similarly, the asymptotic solution and its derivative in region III at $z = L$ are given by

$$\vec{\Psi}_{\text{III}}(L) = \mathbf{E}_+(L) \vec{T} \quad (24)$$

$$\vec{\Psi}'_{\text{III}}(L) = \mathbf{E}'_+(L) \vec{T} \quad (25)$$

where

$$\vec{T} = (T_1, T_2, \dots, T_N) \quad (26)$$

$\mathbf{E}_+(L)$ and $\mathbf{E}'_+(L)$ are diagonal matrices with $[\mathbf{E}_+(L)]_{j,j} = \exp(i\beta_j L)$ and $[\mathbf{E}'_+(L)]_{j,j} = i\beta_j \exp(i\beta_j L)$. The Bloch solution and its derivative in region II at $z = 0$ and $z = L$ are given by

$$\vec{\Psi}_{\text{II}}(0) = \Psi_+(0) \vec{C}^+ + \Psi_-(0) \vec{C}^- \quad (27)$$

$$\vec{\Psi}'_{\text{II}}(0) = \Psi'_+(0) \vec{C}^+ + \Psi'_-(0) \vec{C}^- \quad (28)$$

$$\vec{\Psi}_{\text{II}}(L) = \Psi_+(L) \vec{C}^+ + \Psi_-(L) \vec{C}^- \quad (29)$$

$$\vec{\Psi}'_{\text{II}}(L) = \Psi'_+(L) \vec{C}^+ + \Psi'_-(L) \vec{C}^- \quad (30)$$

where Ψ_\pm are matrices of coefficients of ideal modes $\Phi_j^{(0)}$ in the expansion of the Bloch solutions Ψ_j^\pm , and \vec{C}^\pm are vectors of unknown coefficients

$$\vec{C}^\pm = (C_1^\pm, C_2^\pm, \dots, C_N^\pm) \quad (31)$$

$$[\Psi_\pm(0)]_{i,j} = D_{i,j}^\pm \quad (32)$$

$$\begin{aligned} \Psi'_\pm(0) = \pm i & \begin{pmatrix} k_1 D_{11}^\pm & \dots & k_N D_{1N}^\pm \\ \vdots & \ddots & \vdots \\ k_1 D_{N1}^\pm & \dots & k_N D_{NN}^\pm \end{pmatrix} \\ & + \begin{pmatrix} D'_{11}^\pm & \dots & D'_{1N}^\pm \\ \vdots & \ddots & \vdots \\ D'_{N1}^\pm & \dots & D'_{NN}^\pm \end{pmatrix} \end{aligned} \quad (33)$$

$$\Psi_\pm(L) = \begin{pmatrix} e^{\pm ik_1 L} D_{11}^\pm & \dots & e^{\pm ik_N L} D_{1N}^\pm \\ \vdots & \ddots & \vdots \\ e^{\pm ik_1 L} D_{N1}^\pm & \dots & e^{\pm ik_N L} D_{NN}^\pm \end{pmatrix} \quad (34)$$

and

$$\begin{aligned} \Psi'_{\pm}(L) = & \pm i \begin{pmatrix} k_1 e^{\pm i k_1 L} D_{11}^{\pm} & \cdots & k_N e^{\pm i k_N L} D_{1N}^{\pm} \\ \vdots & \ddots & \vdots \\ k_1 e^{\pm i k_1 L} D_{N1}^{\pm} & \cdots & k_N e^{\pm i k_N L} D_{NN}^{\pm} \end{pmatrix} \\ & + \begin{pmatrix} e^{\pm i k_1 L} D'_{11}{}^{\pm} & \cdots & e^{\pm i k_N L} D'_{1N}{}^{\pm} \\ \vdots & \ddots & \vdots \\ e^{\pm i k_1 L} D'_{N1}{}^{\pm} & \cdots & e^{\pm i k_N L} D'_{NN}{}^{\pm} \end{pmatrix} \end{aligned} \quad (35)$$

where D_{ij}^{\pm} is the coefficient of the ideal mode j in the expansion of the Bloch solution i such that

$$\Phi_i^{\pm}(x, z) = \sum_j D_{ij}^{\pm}(z) \Phi_j^{(0)}(x). \quad (36)$$

The length of the periodic structure L is chosen to be equal to an integral number of periods, and, therefore, $D_{ij}^{\pm}(z=0) = D_{ij}^{\pm}(z=L) \equiv D_{ij}^{\pm}$. From the requirement that the solution (and its derivative) in each region are equal at the region boundary, we obtain

$$\begin{aligned} \vec{\Psi}_I(0) &= \vec{\Psi}_{II}(0) \\ \vec{\Psi}'_I(0) &= \vec{\Psi}'_{II}(0) \\ \vec{\Psi}_{II}(L) &= \vec{\Psi}_{II}(L) \\ \vec{\Psi}'_{II}(L) &= \vec{\Psi}'_{II}(L). \end{aligned} \quad (37)$$

Solving the four vector equations of (37), one can easily calculate the Bloch wave coefficients \vec{C}^{\pm} , the reflection amplitudes \vec{R} , and the transmission amplitudes \vec{T} that correspond to the incoming wave of interest.

The main numerical difficulty of this scheme is the calculation of the Bloch solutions which requires several diagonalizations of the Bloch operator matrix [see (11)]. However, once the Bloch solutions are calculated, the transmission and reflection amplitudes can be easily calculated for *any* length of the periodic structure, since it is important only at the numerically simple matching stage. Therefore, the advantages of this approach are profound when the periodicity region (II in Fig. 1) includes many periods. Moreover, in this case, the Bloch solutions (obtained under the assumption of an infinite number of periods) provide a good approximation to the actual properties of light propagation in a finite periodic structure. The example of such a system is the optical coupler discussed in [20].

In the next section, we implement the numerical method described in Section II to the intermediate-mode-assisted coupler which was formerly studied in the framework of the paraxial approximation [20].

III. INTERMEDIATE-MODE-ASSISTED OPTICAL DIRECTIONAL COUPLER

Directional couplers are important for many applications in optical communications and integrated optics. In its simplest form, a directional coupler consists of two parallel dielectric waveguides in close proximity. The power coupling is based on optical interference, or beating, between the modal fields of the waveguides, such that a light wave launched into one of the waveguides can be coupled completely into the opposite guide [1], [2].

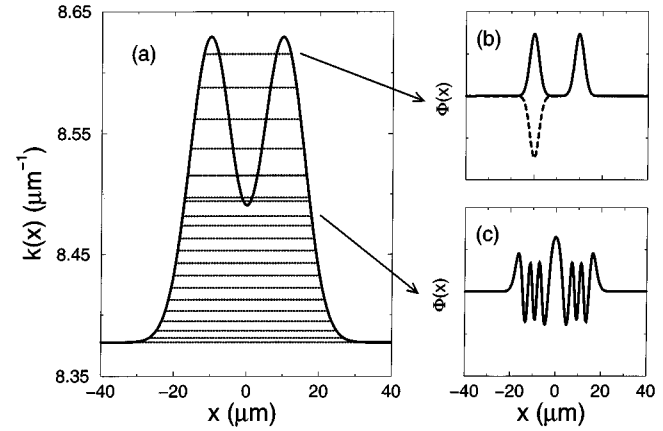


Fig. 2. (a) $k(x) = (\omega/c)n(x)$ function for $n(x)$ as defined in (38) for $n_0 = 2.0$, $n_1 = 2.06$, $\lambda = 1.5 \mu\text{m}$ (free space wavelength), $x_1 = -10 \mu\text{m}$, $x_2 = 10 \mu\text{m}$, and $a = 0.015 \mu\text{m}^{-2}$. Horizontal lines stand for the propagation constants β_j [see (4)]. For first five lines ($k(x=0) < \beta_j < kn_1$), each line corresponds to two almost degenerate β_j values (associated with even-odd pair of modes). (b) The first even-odd pair of lowest order modes as a function of x . (c) Thirteenth trapped mode as a function of x .

The exchange of power between two identical coupled waveguides with embedded periodic structure along the z direction was studied in [20]. It was shown that, due to special symmetry properties of optical modes, a strong enhancement or a total suppression of power exchange can be obtained. The power exchange control is realized by the interaction of the lowest order waveguide modes with high-order modes. An incoming wave which is localized in one waveguide and is a linear combination of even and odd modes interacts with a third high-order mode, such that two modes with the same symmetry are strongly coupled. The mode coupling is induced by a periodic grating with a long period and small amplitude. The numerical study in [20] was performed in the framework of the paraxial approximation. When the paraxial wave equation is solved, the reflected waves are neglected and the wavevectors of the forward-propagating waves are not exact. In this section, we compare the exact results obtained using the method described in Section II with the results obtained in the framework of the paraxial approximation.

We consider a waveguide structure composed of two identical Gaussian graded waveguides in proximity to each other, i.e.,

$$n^2(x) = (n_1^2 - n_0^2) \left(e^{-a(x-x_1)^2} + e^{-a(x-x_2)^2} \right) + n_0^2. \quad (38)$$

The $k(x) = (\omega/c)n(x)$ function for $n_0 = 2.0$, $n_1 = 2.06$, $\lambda = 1.5 \mu\text{m}$ (free space wavelength), $x_1 = -10 \mu\text{m}$, $x_2 = 10 \mu\text{m}$, and $a = 0.015 \mu\text{m}^{-2}$ is plotted in Fig. 2(a). The propagation constants β_j [see (4)] of bound modes obtained for such an index of refraction distribution are shown as horizontal lines. The trapped modes of the structure with the refractive index profile shown in Fig. 2(a) can be divided into two classes. One is the modes with propagation constants higher than $k(x=0)$ [two modes with the highest β_j are plotted in Fig. 2(b)]. These modes form even-odd pairs such that the difference in propagation constants within each pair is much smaller than the differences between the pairs. Such modes are localized near the waveguides centers (x_1 and x_2) and essentially vanish in between ($x=0$). The other type is high-order trapped modes

with $k_0 < \beta_j < k(x=0)$, where k_0 is the wavevector in the uniform cladding. These modes do not form pairs and are “common” modes of the two waveguides, i.e., they are spread over the two-waveguide structure. One such mode is plotted in Fig. 2(c).

For a z -independent refractive index, the reflected waves are not important and the solution of the wave equation (1) is given by

$$\Psi(x, z) = \sum_j C_j^{(0)} e^{i\beta_j z} \Phi_j^{(0)}(x) \quad (39)$$

where $C_j^{(0)} = \int_{A_\infty} \Phi_j^{(0)}(x) \Psi^{(i)}(x, 0) dx$ is a projection of the incoming wave $\Psi^{(i)}(x, 0)$ onto the trapped mode j and A_∞ is the infinite cross section. If one takes as an incoming wave at $z = 0$ a linear combination of the two lowest order trapped modes (Fig. 2(b)) such that the field is localized in the right waveguide (sum field)

$$\Psi^{(i)}(x, 0) = \Psi_R(x) = \frac{1}{\sqrt{2}} \Phi_1^{(0)}(x) + \frac{1}{\sqrt{2}} \Phi_2^{(0)}(x) \quad (40)$$

then, because of the orthonormality of $\Phi_j^{(0)}$, the z -dependence of the optical wave $\Psi(x, z)$ is given by

$$\Psi(x, z) = \frac{1}{\sqrt{2}} e^{i\beta_1 z} \Phi_1^{(0)}(x) + \frac{1}{\sqrt{2}} e^{i\beta_2 z} \Phi_2^{(0)}(x). \quad (41)$$

A difference field localized in the left waveguide is defined as

$$\Psi_L(x) = \frac{1}{\sqrt{2}} \Phi_1^{(0)}(x) - \frac{1}{\sqrt{2}} \Phi_2^{(0)}(x). \quad (42)$$

Since $\Psi_R(x)$ and $\Psi_L(x)$ are spatially far apart one can define the directional coupling probability as

$$P(z) = \left| \int_{A_\infty} \Psi(x, z) \Psi_L(x) dx \right|^2. \quad (43)$$

Substituting (41) into (43) one obtains that the directional coupling probability is given by

$$P(z) = \frac{1}{2} - \frac{1}{2} \cos((\beta_2 - \beta_1)z). \quad (44)$$

Therefore, the light power (defined as $|\int_{A_\infty} \Psi(x, z) dx|^2$), initially localized in the right waveguide, couples to the left one and the complete exchange of light power is obtained at $z_b = \pi/(\beta_1 - \beta_2)$ (beat length) [1], [2]. In our studied case, β_j values corresponding to $\Phi_1^{(0)}(x)$ and $\Phi_2^{(0)}(x)$ are very close and the splitting $\Delta_0 = \beta_2 - \beta_1$ is very small: $\Delta_0 = 5.95 \times 10^{-10} \mu\text{m}^{-1}$, which results in a beat length of more than 5 km. In [20], it was shown that the directional coupling can be enhanced by orders of magnitude by using an embedded periodic structure. Unlike grating assisted directional couplers [1], [4]–[11], in which the periodic thickness variations are applied to a nonsynchronous coupler (e.g., in coupled waveguides with nonidentical core refractive indices), we study the case in which the periodic structure is used to enhance the directional coupling of synchronous couplers with very large beat lengths. In this case, in the absence of the grating, the directional coupling is negligible and, therefore, this coupling mechanism can be used both as an optical coupler and as an optical switch. The directional coupling

enhancement is based on the coupling of the almost degenerate lowest order modes with a high-order mode. Since these two modes have different symmetry and the third mode has the same symmetry as one of them, only one of the lowest order modes is coupled. As a result, the splitting between the wavevectors of the two almost degenerate modes grows and the beat length is significantly shortened. The coupling is realized by an embedded periodic structure, the period of which is chosen to couple the lowest order modes with a specific high-order mode. In our studied case, the period of the refractive index variations $\Lambda = 50 \mu\text{m}$ that corresponds to a coupling between the two lowest order modes shown in Fig. 2(b) and the 13th-order mode shown in Fig. 2(c).

The embedded periodic structure can be induced either by not using real-time methods—a fixed periodic structure and a possible control of the structure functionality is gained by changing the refractive index profile of the waveguide structure using the electrooptic effect—or by using real-time methods such as acoustic waves that are launched into the media to produce transient pressure waves.

We consider a z -dependent refractive index model such that

$$\begin{aligned} n^2(x, z) &= n^2 \left(x + \alpha_0 \sin \left[\frac{2\pi}{\Lambda} z \right] \right) \\ &= (n_1^2 - n_0^2) \left(e^{-a[x-x_1(z)]^2} + e^{-a[x-x_2(z)]^2} \right) + n_0^2 \end{aligned} \quad (45)$$

where $x_{1,2}(z) = x_{1,2} + \alpha_0 \sin([2\pi/\Lambda]z)$. In this model, the indices of refraction do not change as a function of z , but the structure is bent periodically with a period Λ and an amplitude α_0 . In contrast to the well-known case of Bragg reflectors, the directional coupling mechanism is based on a moderate grating, i.e., a grating with a period which is much larger than the wavelength and an amplitude which is small compared to the transverse dimensions of the waveguide structure. If both these conditions are kept, we can assume that back-reflection effects are small and Bloch waves $\Phi_k(x, z)$ [see (8) and (10)] are very similar to the ideal modes of the uniform waveguide [see (4)]. In this case, the solution of the wave equation (1) can be approximated by a linear combination of two Bloch waves corresponding to two lowest order modes that constitute the incoming wave $\Psi^{(i)}(x, 0)$ defined in (40)

$$\Psi_{\text{II}}(x, z) \simeq \frac{1}{\sqrt{2}} e^{ik_1 z} \Phi_{k_1}(x, z) + \frac{1}{\sqrt{2}} e^{ik_2 z} \Phi_{k_2}(x, z) \quad (46)$$

where Φ_{k_1} and Φ_{k_2} are Bloch waves corresponding to the two lowest order modes $\Phi_1^{(0)}(x)$ and $\Phi_2^{(0)}(x)$. In this case, the beat length is inversely proportional to the splitting between the Bloch wavevectors

$$\Delta = |k_1 - k_2|. \quad (47)$$

For moderate gratings, one can use the paraxial approximation for the solution of the wave equation [20]. In the framework of this approximation, one assumes that the solution of the wave equation is given by

$$\Psi(x, z) = e^{ik_0 z} \Phi(x, z) \quad (48)$$

where k_0 is the wavevector in the cladding and $\Phi(x, z)$ is a weakly z -dependent function. Substituting (48) into (1) and neglecting the second derivative of $\Phi(x, z)$ with respect to z , we obtain

$$\left[2ik_0 \frac{\partial}{\partial z} - k_0^2 + \nabla_x^2 + \frac{\omega^2}{c^2} n^2(x, z) \right] \Phi(x, z) = 0. \quad (49)$$

For a z -independent refractive index, the solution of (49) is given by

$$\Phi(x, z) = e^{ik_0 d_j z} \Phi_j^{(0)}(x) \quad (50)$$

such that

$$\left[\nabla_x^2 + \frac{\omega^2}{c^2} n^2(x) \right] \Phi_j^{(0)}(x) = k_0^2 (1 + 2d_j) \Phi_j^{(0)}(x) \quad (51)$$

and the solution of the wave equation (1) is

$$\Psi_j(x, z) = e^{ik_0(1+d_j)z} \Phi_j^{(0)}(x). \quad (52)$$

The relation between propagation constants β_j , defined in (4), and d_j values defined in (51) is given by

$$\beta_j = k_0 \sqrt{1 + 2d_j}. \quad (53)$$

By comparing the exact solution of the wave equation given in (3) with the approximate solution in (52), one can see that in the framework of the paraxial approximation the back-traveling waves $\exp(-i\beta_j z) \Phi_j^{(0)}(x)$ are neglected and the propagation constants of the forward-traveling waves are approximated by

$$\beta_j = k_0(1 + d_j). \quad (54)$$

(54) is an approximation to (53) that is correct up to a second-order term d_j^2 . d_j is a dimensionless eigenvalue of [see (51)]

$$\left[\frac{1}{2k_0^2} \nabla_x^2 + \frac{1}{2} \left(\frac{n^2(x)}{n_0^2} - 1 \right) \right] \Phi_j^{(0)} = d_j \Phi_j^{(0)} \quad (55)$$

and it measures the relative difference between the propagation constants and the wavevector in the cladding k_0 . This difference is small for a single-mode waveguide, but can be quite large for the lowest order modes of a multi-mode one.

The paraxial approximation provides very significant numerical advantages. First, it transforms the wave equation into a propagation problem which can be solved efficiently by the beam propagation method [23], [24]. Second, when moderate periodic structures are studied and Bloch theorem is applied to (49), then the Bloch waves can be calculated in a simpler fashion. For a periodic refractive index the solution of (49) is given by

$$\Phi_j(x, z) = e^{ik_0 \epsilon_j z} \tilde{\Phi}_j(x, z) \quad (56)$$

where $\tilde{\Phi}_j(x, z) = \tilde{\Phi}_j(x, z + \Lambda)$ and

$$\left[\frac{i}{k_0} \frac{\partial}{\partial z} + \frac{1}{2k_0^2} \nabla_x^2 + \frac{1}{2} \left(\frac{n^2(x, z)}{n_0^2} - 1 \right) \right] \tilde{\Phi}_j(x, z) = \epsilon_j \tilde{\Phi}_j(x, z). \quad (57)$$

In contrast to (10), when the paraxial approximation is used, the Bloch waves $\Phi_j(x, z)$ and eigenphases ϵ_j are the eigenvectors

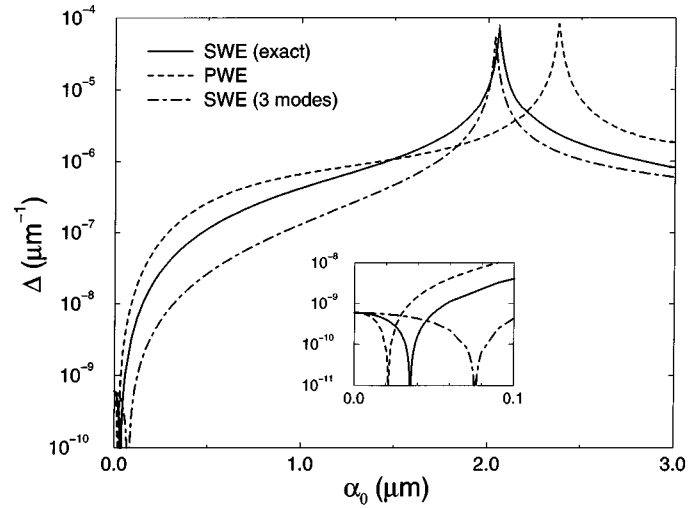


Fig. 3. The splitting between the two Bloch wavevectors (on a logarithmic scale) that corresponds to the two lowest order optical modes as a function of the grating amplitude for the grating period $\Lambda = 50 \mu\text{m}$ (see (45)). The solid line represents the splitting value as obtained from the solution of the scalar wave equation [see (10) and (47)]. The dashed line represents the approximate value of the splitting as obtained from the solution of the paraxial wave equation [see (57) and (59)]. The dotted-dashed line represents the splitting value as obtained from the solution of the scalar wave equation when only three corresponding ideal modes are used to describe the Bloch waves. The inset is a zoomed view near $\alpha_0 = 0$ to show the splitting value of the uniform waveguide.

and the eigenvalues of the Floquet–Bloch operator in (57). A typical eigenvalue problem in (57) can be solved by straightforward diagonalization methods or, more efficiently, by calculating the one-period propagator [20], [25]. The approximate solution of the wave equation is given by

$$\Psi(x, z) = \sum_j c_j^+ e^{ik_0(1+\epsilon_j)z} \tilde{\Phi}_j(x, z) \quad (58)$$

where $c_j^+ = \int_{A_\infty} \Phi_j^{(0)}(x) \Psi(x, 0) dx$ is a projection of the initial state $\Psi(x, 0)$ onto the trapped mode j and A_∞ is the infinite cross section. In this case, the beat length is inversely proportional to the splitting between the eigenphases ϵ_j

$$\Delta = k_0 |\epsilon_1 - \epsilon_2|. \quad (59)$$

Since the Bloch formalism allows us to calculate the Bloch wavevectors (eigenphases) explicitly, we first study the dependence of the phases on parameters of the grating. The splitting between the wavevectors corresponding to the two lowest order modes of the waveguide structure as a function of the grating amplitude is shown in Fig. 3. As one can see that the wavevectors splitting grows very fast as the amplitude of the grating amplitude is increased. In addition, for specific value of α_0 , the splitting exhibits a maximal value associated with a peak in the plot. In the framework of the paraxial approximation, one can use perturbation theory to estimate the wavevectors' splitting [20]. Perturbation theory with the one-period average effective refractive index as a zeroth-order approximation [20], [26] shows that the splitting growth is due to the nonresonant and resonant coupling between one of the lowest order modes and a high-order mode. To illustrate this, we plot three relevant Bloch wavevectors k_j as a function of α_0 in Fig. 4. Two of them (labeled k_1 and k_2) form a pair of almost degenerate

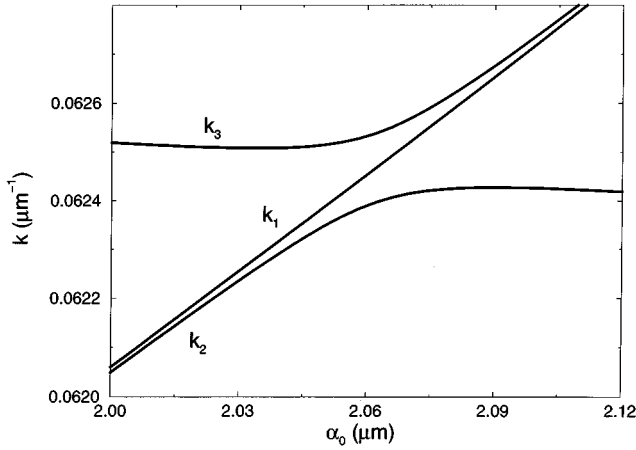


Fig. 4. The Bloch wavevectors k_j as a function of the grating amplitude α_0 as obtained from (10). The plot is zoomed near $\alpha_0 = 2.0631 \mu\text{m}$ associated with the maximal value of the wavevectors' splitting shown in Fig. 2. The trajectories of the wavevectors labeled k_1 and k_2 belong to two Bloch waves which correspond to two almost degenerate trapped modes $\Phi_1^{(0)}(x)$ and $\Phi_2^{(0)}(x)$ shown in Fig. 2(b). The wavevector trajectory labeled k_3 belongs to the third Bloch wave which correspond to the 13th trapped mode $\Phi_{13}^{(0)}(x)$ shown in Fig. 2(c).

Bloch waves that corresponds to the even-odd pair of modes with highest β_j , shown in Fig. 2(b). The third one (labeled k_3) corresponds to one of the Bloch waves that evolved from the high-order mode shown in Fig. 2(c). The two almost degenerate Bloch waves have a different parity and the third has the same parity as one of them. Since the trajectories of wavevectors that correspond to Bloch waves with identical parity cannot cross, the avoided crossing with only one of them occurs. As a result, the splitting between the two almost degenerate wavevectors grows and it has a maximal value at the avoided crossing point, at which the two states with the same parity are resonantly coupled. Since the enhancement and suppression of directional coupling is based on interaction of three Bloch waves, one can attempt to use only three modes of the uniform waveguide to model it. This would enable, for example, the use of the coupled-mode approach based on a coupling of only three ideal modes. However, since initially the wavevector splitting is very small, the three-mode model is able to give only a qualitative picture, but is unable to give quantitatively correct results for the fast change of the wavevectors' difference. The wavevectors' difference obtained when only three ideal modes are used to describe the Bloch waves is shown in Fig. 3 by the dotted-dashed line. As one can see, the three-mode model can give a relatively good prediction for the value of the grating amplitude for which the wavevectors' splitting gets a maximal value. However, far from the avoided crossing point, the three-mode model gives the wavevectors' splitting that is up to 10 times smaller than the correct result. Therefore, the coupling distance obtained with only three-modes is up to 10 times larger than the correct one. Similar results are obtained in the framework of the paraxial approximation. In this case, the splitting growth is relatively similar to the correct one (shown by a dashed line in Fig. 3). However, the value of the grating amplitude α_0 for which the resonant coupling is obtained is not correct when the paraxial approximation is used. The discrepancy is due to the fact that the approximation for the wavevectors given in (54) is a poor one for the lowest

order modes of a multimode waveguide structure. Since, in our case, the two almost degenerate lowest order modes are the relevant ones, the paraxial approximation gives a poor estimation for the grating amplitude for which the resonant coupling is obtained.

In order for the splitting $\Delta = |k_1 - k_2|$ to describe the directional coupling enhancement, we need two conditions to be fulfilled. First, reflected waves should not be important and, second, two Bloch waves should dominate the expansion of the solution of the wave equation in the region where the refractive index is periodic. In this context, two cases can be considered. One is the nonresonant coupling between the lowest order mode and a high-order mode. In this case, the wavevectors splitting is not maximal, but only two Bloch waves contribute to the solution of the wave equation in the region where the refractive index is periodic. Second, in the resonant-coupling case in which the splitting is maximal, one of the lowest order modes is mixed with the high-order mode. Therefore, in resonance, the optical wave is expected to be given by a linear combination of three Bloch waves. We calculate the coefficients of the forward/backward propagating Bloch waves and transmission/reflection coefficients for both cases using the matching procedure described in Section II. The incoming wave vector [see (18)] is defined as

$$\vec{\Psi}_i(0) = \left(\frac{1}{\sqrt{2}}, \frac{1}{\sqrt{2}}, 0, \dots, 0 \right) \quad (60)$$

which corresponds to the sum field given by (40).

The results of the matching procedure for the nonresonant coupling case for $\alpha_0 = 1.7 \mu\text{m}$ are shown in Fig. 5. The length of the grating is chosen to be equal to the beat length value corresponding to the wavevectors' splitting shown in Fig. 3: $L = \pi/|k_1 - k_2|$. As one can see in Fig. 5(a), the coefficients of the back-propagating Bloch waves, C^- , are much smaller than these of the forward propagating ones, C^+ . Therefore, in this case, the paraxial approximation that takes into account only forward-propagating Bloch waves is very good. In addition, as one can see in Fig. 5(a), the coefficients of the first two Bloch waves that correspond to the two almost degenerate lowest order modes, C_1^+ and C_2^+ , are much larger than the coefficients of other Bloch waves. Thus, a two-wave approximation given in (46) is also a good one. Therefore, the beat length is inversely proportional to the splitting between wavevectors k_1 and k_2 . As one can see in Fig. 3, $\Delta = |k_1 - k_2|$ has grown from $\sim 10^{-9}$ to $\sim 10^{-6}$. Therefore, in the region where the refractive index is periodic, the directional coupling is enhanced by more than three orders of magnitude. An additional important piece of information is the transmission and reflection coefficients that describe the solution of the wave equation before and after the grating. As one can see in Fig. 5(b), the reflection coefficients are negligible and the transmitted waves are mainly $\Phi_1^{(0)}$ and $\Phi_2^{(0)}$. Thus, the coupling between the modes of the incoming wave and other modes of the waveguide is small and the directional coupling is very close to 100%. In our studied case, the nonresonant coupling leads to a beat length which is still very large ($\sim 2 \text{ m}$). However, in this case, one can use the nonresonant coupling mechanism to transfer a small portion of the light power from one waveguide to another in a controllable fashion, where the control is gained by varying the length of the periodic structure.

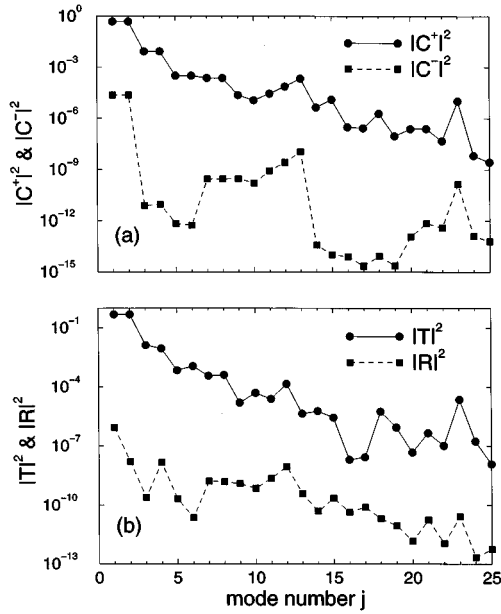


Fig. 5. The results of the matching procedure as obtained from (37) for the incoming wave defined in (60) and the grating period $\Lambda = 50 \mu\text{m}$, the grating amplitude $\alpha_0 = 1.7 \mu\text{m}$, and the length of the periodic structure $L = 1.95 \text{ m}$. (a) Coefficients of the Bloch waves (see (31)) on a logarithmic scale versus the number of the ideal mode $\Phi_j^{(0)}$ to which they correspond. Dots connected by a solid line correspond to the forward-propagating Bloch waves and squares connected by a dashed line correspond to the backward-propagating Bloch waves. (b) Transmission coefficients (dots connected by a solid line) (see (26)) and reflection coefficients (squares connected by a dashed line) (see (23)) of different ideal modes versus the mode number.

Moreover, if one would choose a synchronous coupler with a relatively small beat length without a periodic structure, then, using the nonresonant coupling induced by a periodic structure, one could reduce the beat length to an even smaller value.

The beat length is further shortened by the resonant coupling mechanism. The results of the matching procedure for the resonant enhancement are shown in Fig. 6. As one can see in Fig. 6(b), the coefficients of the three forward-propagating Bloch waves, C_1^+ , C_2^+ and C_{13}^+ , are much larger than all other coefficients. In fact, $|C_1^+|^2 \simeq 0.5$ and $|C_2^+|^2 \simeq |C_{13}^+|^2 \simeq 0.25$. Therefore, in the case of a resonant mode coupling, one can write the optical wave in the region where the refractive index is periodic as

$$\Psi(x, z) \simeq \frac{1}{\sqrt{2}} e^{ik_1 z} \Phi_{k_1}(x, z) + \frac{1}{2} e^{ik_2 z} \Phi_{k_2}(x, z) + \frac{1}{2} e^{ik_3 z} \Phi_{k_3}(x, z) \quad (61)$$

where $\Phi_{k_3}(x, z)$ is the Bloch wave that corresponds to the third high-order mode ($\Phi_{13}^{(0)}$, in our case) that is coupled to the Bloch wave of the same parity $\Phi_{k_2}(x, z)$. One can rearrange (61) in the following form:

$$\Psi(x, z) \simeq e^{ik_1 z} \frac{1}{\sqrt{2}} \left(\Phi_{k_1} + e^{i(k_2 - k_1)z} \Phi_{k_{2,3}} \right) \quad (62)$$

where

$$\Phi_{k_{2,3}} \equiv \frac{1}{\sqrt{2}} \left(\Phi_{k_2} + e^{i(k_3 - k_2)z} \Phi_{k_3} \right). \quad (63)$$

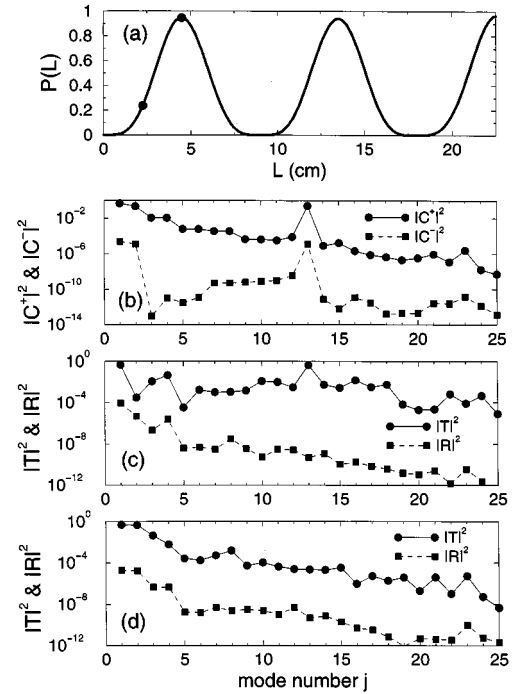


Fig. 6. The results of the matching procedure as obtained from (37) for the incoming wave defined in (60), the grating period $\Lambda = 50 \mu\text{m}$, and the grating amplitude $\alpha_0 = 2.0631 \mu\text{m}$ corresponding to the peak in the $\Delta(\alpha_0)$ function shown in Fig. 3. (a) The directional coupling probability defined in (43) as a function of the length of the periodic structure. (b) The same as in Fig. 5(a) for $L = 2.25 \text{ cm}$. (c) The same as in Fig. 5(b) for $L = 2.25 \text{ cm}$ corresponding to the first filled circle in the $P(z)$ plot in (a). (d) The same as in Fig. 5(b) for $L = 4.5 \text{ cm}$ corresponding to the second filled circle in the $P(z)$ plot in (a).

$\Phi_{k_2}(x, z)$ and $\Phi_{k_3}(x, z)$ are Bloch waves that correspond to ideal modes $\Phi_2^{(0)}(x)$ and $\Phi_{13}^{(0)}(x)$ that are resonantly coupled, such that

$$\Phi_{k_2}(x, 0) \simeq \frac{1}{\sqrt{2}} \left(\Phi_2^{(0)}(x) + \Phi_{13}^{(0)}(x) \right) \quad (64)$$

and

$$\Phi_{k_3}(x, 0) \simeq \frac{1}{\sqrt{2}} \left(\Phi_2^{(0)}(x) - \Phi_{13}^{(0)}(x) \right). \quad (65)$$

Hence,

$$\frac{1}{\sqrt{2}} \left(\Phi_{k_2}(x, 0) + \Phi_{k_3}(x, 0) \right) \simeq \Phi_2^{(0)}(x) \quad (66)$$

and

$$\frac{1}{\sqrt{2}} \left(\Phi_{k_2}(x, 0) - \Phi_{k_3}(x, 0) \right) \simeq \Phi_{13}^{(0)}(x). \quad (67)$$

From (66) and (67), one obtains that $\Phi_{k_{2,3}}(x, z)$ defined in (63) oscillates between $\Phi_2^{(0)}(x)$ and $\Phi_{13}^{(0)}(x)$ with a period $\pi/(k_3 - k_2)$. Therefore, at $z = 2m\pi/(k_3 - k_2)$, $m = 0, 1, 2, \dots$, the third high-order mode does not contribute to the optical wave, which, to a good approximation, is given by a linear combination of two Bloch waves that correspond to the two lowest order modes. The Bloch function $\Phi_{k_1}(x, z)$ is uncoupled because of

symmetry and, therefore, $\Phi_{k_1}(x, 0) \simeq \Phi_1^{(0)}(x)$. Thus, the optical wave at the beat length $z_b = 2m\pi/(k_3 - k_2)$, $m = 1, 2, \dots$ is approximately given by

$$\Psi(x, z_b) \simeq e^{ik_1 z_b} \frac{1}{\sqrt{2}} \left(\Phi_1^{(0)} + e^{i2m\pi(k_2 - k_1)/(k_3 - k_2)} \Phi_2^{(0)} \right). \quad (68)$$

At the avoided crossing, however, there exists a special relation between the Bloch wavevectors (see Fig. 4), i.e.,

$$k_3 - k_1 = k_1 - k_2 \quad (69)$$

and, therefore,

$$k_3 - k_2 = -2(k_2 - k_1). \quad (70)$$

Using (70) and (68), one obtains

$$\Psi(x, z_b) \simeq e^{ik_1 z_b} \frac{1}{\sqrt{2}} \left(\Phi_1^{(0)} - \Phi_2^{(0)} \right). \quad (71)$$

Consequently, although three Bloch waves contribute to the solution of the wave equation, at $z_b = m\pi/(k_1 - k_2)$, $m = 0, 1, 2, \dots$ the optical wave is to a good approximation given by $\Psi_L(x)$ defined in (42). Hence, at this distance, a complete directional coupling is obtained and the beat length is inversely proportional to the splitting between wavevectors of two Bloch waves [see (47)]. Since the splitting grows significantly due to the resonance coupling between Bloch waves, the directional coupling is enhanced by many orders of magnitude. The directional coupling probability defined in (43) for the resonant enhancement case is shown in Fig. 6(a). As one can see, an almost total power transfer from one waveguide to another is obtained after $z_b = 4.5$ cm. This is more than five orders of magnitude faster than without the periodic structure. The transmission and reflection coefficients for two different lengths of the periodic structure are shown in Fig. 6(c) and (d). In Fig. 6(c), the length of the periodic structure $L = 2.25$ cm that corresponds to the half a beat length $z_b/2 = \pi/(k_3 - k_2)$ at which one of the lowest order modes does not contribute and $\Psi_{k_{2,3}}(x, 0) \simeq \Psi_{13}^{(0)}$ [see (63)]. Indeed, as one can see in Fig. 6(c), if one chooses the length of the periodic structure such that $L = z_b/2$, then the optical wave after the grating is given mainly by a linear combination of $\Phi_1^{(0)}$ and $\Phi_{13}^{(0)}$. However, if the length of the periodic structure is equal to the beat length defined in (47) [see Fig. 6(d)], then the optical wave after the grating is given mainly by a linear combination of the two lowest order modes $\Phi_1^{(0)}$ and $\Phi_2^{(0)}$. In addition, because of the grating, one of the modes ($\Phi_2^{(0)}$) changes its phase, such that the sum field transforms to the difference field and the directional coupling takes place.

One should notice that, in general, the coefficients of the Bloch waves C^\pm also depend on the length of the periodic structure L . However, for the moderate grating case the dependence is very weak and can be neglected. This is related to the fact that for the moderate grating case the paraxial approximation is a good one. In the framework of the paraxial approximation the coefficients of forward-propagating Bloch waves are determined by the overlap integral between the initial state $\Psi(x, z = 0)$ and the Bloch waves [see (58)]. Since the Bloch waves are

periodic, the c_j^+ coefficients do not depend on L if it is given by an integral number of the grating periods. Although it is difficult to obtain a similar condition for C^+ calculated from the matching procedure [see (37)], for moderate gratings, the correspondence between the coefficients of exact Bloch waves and approximate Bloch waves obtained from the paraxial approximation is preserved.

In the previous examples, the reflected waves were not important, and the paraxial approximation could provide a physically correct picture for the behavior of the optical wave. This is due to the fact that a moderate grating was considered, i.e., a grating with a period much larger than the wavelength and a small grating amplitude. To illustrate the efficiency of the numerical method described in Section II for the case where the paraxial approximation cannot be applied, we consider a grating with a period comparable to the wavelength. The directional coupling enhancement described in this section is based on the mode coupling induced by the periodic structure. A periodic structure with a large period is chosen such that two forward-propagating waves are coupled, i.e.,

$$\Lambda \simeq \frac{\pi}{\beta_2 - \beta_{13}} \quad (72)$$

where β_2 is the propagation constant of one of the almost degenerate lowest order modes and β_{13} is the propagation constant of the 13th high-order mode. A different kind of mode coupling can be achieved by choosing

$$\Lambda \simeq \frac{\pi}{\beta_2 + \beta_{13}}. \quad (73)$$

In this case, the forward-propagating optical mode $\Phi_2^{(0)}$ is coupled to the backward-propagating optical mode $\Phi_{13}^{(0)}$. The main difference is that the grating period given by (73) is much smaller than that given by (72) and the reflected waves become important. Moreover, for a small grating period, the dispersion relation $\omega(k)$ has a structure which does not appear when the grating period is much larger than the wavelength. The dispersion relation of the periodic structure given by (45) for the grating period $\Lambda = 0.36755 \mu\text{m}$ that corresponds to the condition in (73) and $\alpha_0 = 1.544 \mu\text{m}$ is shown in Fig. 7(a). As one can see in Fig. 7(a), two Bloch waves with the same parity are coupled and the avoided crossing between them takes place. As a result, there exists a grating amplitude for which a gap in the $\omega(k)$ values of these two modes is formed. For these grating parameters only one of the three Bloch waves is propagating in the periodic structure, while the other two are not. A similar situation is obtained if one varies the grating amplitude for a fixed wavelength. As one can see in Fig. 7(b), the avoided crossing between the Bloch wavevectors is very different from the one shown in Fig. 4. As the grating amplitude, α_0 , is increased one of the lowest order modes couples to the back-propagating high-order mode. For a certain value of the grating amplitude, the waves are resonantly coupled and they mix. If one further increases α_0 , the two coupled modes disappear and only the uncoupled mode remains. For a certain higher amplitude, however, the two coupled modes return and for even higher α_0 two Bloch waves are decoupled again. The reflection and

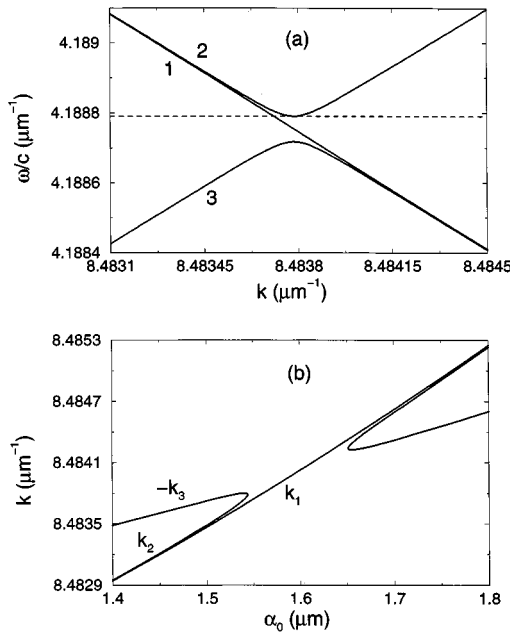


Fig. 7. (a) The dispersion relation $\omega(k)$ defined in (13) for the grating period $\Lambda = 0.36755 \mu\text{m}$ and the grating amplitude $\alpha_0 = 1.544 \mu\text{m}$. The plot is zoomed near $\omega/c = 4.1888 \mu\text{m}^{-1}$ (shown by the dashed line) that corresponds to a free space wavelength $\lambda = 1.5 \mu\text{m}$ used in the intermediate-mode-assisted directional coupling calculations. (b) The Bloch wavevectors k_j as function of the grating amplitude α_0 for $\omega/c = 4.1888 \mu\text{m}^{-1}$. The frequencies labeled 1, 2 in (a) and the wavevectors labeled k_1 and k_2 in (b) belong to two Bloch waves which correspond to two forward-propagating almost degenerate trapped modes $\Phi_1^{(0)}(x)$ and $\Phi_2^{(0)}(x)$ shown in Fig. 2(b). The frequency labeled 3 in (a) and the wavevector labeled $-k_3$ in (b) belongs to the third backward-propagating Bloch wave which corresponds to the 13th trapped mode $\Phi_{13}^{(0)}(x)$ shown in Fig. 2(c).

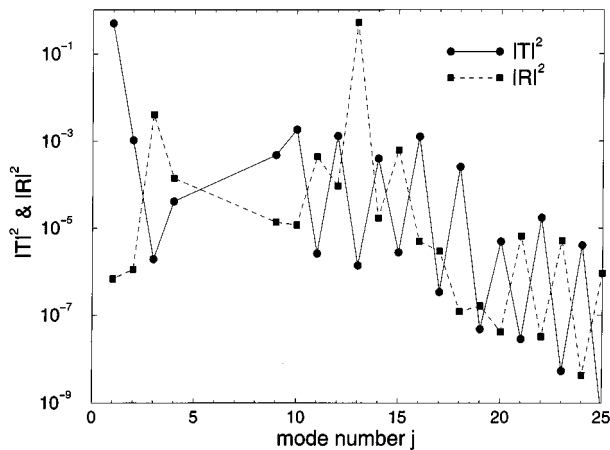


Fig. 8. Transmission coefficients (dots connected by a solid line) [see (26)] and reflection coefficients (squares connected by a dashed line) [see (23)] of different ideal modes versus the mode number for the wavelength $\lambda = 1.5 \mu\text{m}$, the grating period $\Lambda = 0.36755 \mu\text{m}$, and the grating amplitude $\alpha_0 = 1.544 \mu\text{m}$.

transmission coefficients obtained by the matching procedure for a resonant coupling of this form are shown in Fig. 8.

As one can see in Fig. 8, due to the coupling between forward-propagating wave Φ_{k_2} and backward-propagating Φ_{k_3} , a reflected wave $\Psi_{13}^{-(0)}$ is obtained. In addition, for a given wavelength, several modes ($\Phi_j^{(0)}$, $j = 5, 6, 7, 8$) are not guided by the periodic structure. Although a coupling between forward- and backward-propagating Bloch waves shown in Fig. 8 cannot

be used for directional coupling enhancement, it illustrates the applicability of the Bloch wave approach to the cases where reflected waves are important.

IV. CONCLUSIONS

A numerical method for the solution of the wave equation for optical waveguides with periodic inhomogeneities is presented. The method is based on a calculation of the Bloch waves in the region in space where the refractive index is periodic. The transmission and reflection amplitudes are calculated by matching the Bloch waves and the ideal modes of the uniform waveguides before and after the periodicity region. The Bloch wave approach can be efficiently used to study the properties of a waveguide with an embedded periodic structure and to avoid the numerical long-distance propagation through the periodic medium. The method is applied to the intermediate-mode-assisted directional coupler. The exact results obtained using the Bloch wave approach are compared with those obtained in the framework of the paraxial approximation. It is shown that the paraxial approximation provides a physically correct picture, but there is a significant discrepancy between the grating parameters for which an optimal directional coupling is achieved. It is demonstrated that, although the directional coupling features can be explained by interaction of three Bloch waves, three ideal modes only are not sufficient for the correct calculation of the Bloch wavevectors. The Bloch wave approach is shown to be efficient also in the case in which the reflection effects are strong.

REFERENCES

- [1] D. Marcuse, *Theory of Dielectric Optical Waveguides*, 2nd ed. New York, NY: Academic, 1991, and references therein.
- [2] A. W. Snyder and J. D. Love, *Optical Waveguide Theory*. London, U.K.: Chapman & Hall, 1995, and references therein.
- [3] D. Marcuse, *Light Transmission Optics*. Princeton, NJ: Van Nostrand Reinhold, 1984.
- [4] D. L. Lee, *Electromagnetic Principles of Integrated Optics*. New York, NY: Wiley, 1986.
- [5] W. P. Huang and H. A. Haus, "Power exchange in grating-assisted couplers," *J. Lightwave Technol.*, vol. 7, pp. 920–924, 1989.
- [6] R. G. Hunsperger, *Integrated Optics: Theory and Technology*, 2nd ed. Berlin, Germany: Springer Verlag, 1984.
- [7] D. Marcuse, "Directional couplers made of nonidentical asymmetric slabs. Part II: Grating assisted couplers," *J. Lightwave Technol.*, vol. LT-5, pp. 268–273, 1987.
- [8] G. Griffel and A. Yariv, "Frequency response and tunability of grating-assisted directional couplers," *IEEE J. Quantum Electron.*, vol. 27, pp. 1115–1118, 1991.
- [9] W. P. Huang, J. Hong, and Z. M. Mao, "Improved coupled-mode formulation based on composite modes for parallel grating-assisted co-directional couplers," *IEEE J. Quantum Electron.*, vol. 29, pp. 2805–2812, 1993.
- [10] Q. Guo and W. P. Huang, "Polarization-independent optical filters based on co-directional phase-shifted grating-assisted couplers—Theory and designs," *Proc. Inst. Elect. Eng.*, pt. J, vol. 143, pp. 173–177, 1996.
- [11] N.-H. Sun, J. K. Butler, G. A. Evans, L. Pang, and P. Congdon, "Analysis of grating-assisted directional couplers using Floquet–Bloch theory," *J. Lightwave Technol.*, vol. 15, pp. 2301–2315, 1997.
- [12] W. P. Huang, "Coupled-mode theory for optical waveguides: An overview," *J. Opt. Soc. Amer. A*, vol. 11, pp. 963–983, 1994.
- [13] B. Crosignani, P. Diporto, and A. Yariv, "Coupled-mode theory and slowly varying approximation in guided-wave optics," *Opt. Commun.*, vol. 78, pp. 237–239, 1990.
- [14] B. E. Little and H. A. Haus, "A variational coupled-mode theory for periodic waveguides," *IEEE J. Quantum Electron.*, vol. 31, pp. 2258–2264, 1995.

- [15] I. Vorobeichik, N. Moiseyev, and D. Neuhauser, "The effect of the second derivative paraxial term in the scalar Maxwell equation on amplitude losses and reflections in optical fibers," *J. Opt. Soc. Amer. B*, vol. 14, pp. 1208–1213, 1997.
- [16] P. St. J. Russell, "Bloch wave analysis of dispersion and pulse propagation in pure distributed feedback structures," *J. Mod. Opt.*, vol. 38, pp. 1599–1619, 1991.
- [17] —, "Optics of Floquet-Bloch waves in dielectric gratings," *Appl. Phys. B*, vol. 39, pp. 231–246, 1986.
- [18] R. S. Chu and T. Tamir, "Guided-wave theory of light diffraction by acoustic microwaves," *IEEE Trans. Microwave Theory Tech.*, vol. MTT-18, pp. 418–504, 1970.
- [19] C. Elachi, "Waves in active and passive periodic structures: A review," *Proc. IEEE*, vol. 64, pp. 666–1697, 1976.
- [20] I. Vorobeichik, M. Orenstein, and N. Moiseyev, "Intermediate-mode-assisted optical directional couplers via embedded periodic structure," *IEEE J. Quantum Electron.*, vol. 34, pp. 1772–1781, 1998.
- [21] N. W. Ashcroft and N. D. Mermin, *Solid State Physics*. Philadelphia, PA: Saunders College, 1976.
- [22] J. D. Joannopoulos, R. D. Meade, and J. N. Winn, *Photonic Crystals: Molding the Flow of Light*. Princeton, NJ: Princeton Univ. Press, 1995. and references therein.
- [23] M. D. Feit and J. A. Fleck, "Light propagation in graded-index optical fibers," *Appl. Opt.*, vol. 17, pp. 3990–3996, 1978.
- [24] —, "Calculation of dispersion in graded-index multi-mode fibers by a propagating beam method," *Appl. Opt.*, vol. 18, pp. 2843–2849, 1978.
- [25] I. Vorobeichik, U. Peskin, and N. Moiseyev, "Modal losses and design of modal irradiance patterns in an optical fiber by the complex (t, t') method," *J. Opt. Soc. Amer. B*, vol. 12, pp. 1133–1141, 1995.
- [26] I. Vorobeichik and N. Moiseyev, "Tunneling control by high frequency driving," *Phys. Rev. A*, vol. 59, pp. 1699–1702, 1999.



Alexander M. Kenis was born in Samara, Russia, in 1971. He received the B.A. degree in 1993 and M.Sc. degree in 1996 from the Technion—Israel Institute of Technology, Haifa, Israel. He is currently working toward the Ph.D. degree at the same institution in the study of design of optical devices by means of quantum mechanical approaches and computational methods.



Ilya Vorobeichik was born in St. Petersburg, Russia, in 1971. He received the B.A. and Ph.D. degrees from the Technion—Israel Institute of Technology, Haifa, Israel, in 1994 and 1999, respectively.

His research interests are in the study of electromagnetic wave propagation in nonuniform optical waveguides, laser–matter interaction, and numerical methods.



Nimrod Moiseyev was born in Haifa, Israel, in 1947. He received the B.Sc. degree from Bar-Ilan University, Ramat-Gan, Israel, in 1969, the M.Sc. degree from the Weizmann Institute of Science, Rehovot, Israel, in 1972 and D.Sc. degree from the Technion—Israel Institute of Technology, Haifa, Israel, in 1977.

He joined the department of Chemistry at the Technion in 1979, where he is at present a Professor. He is engaged in research in resonance theory, quantum dynamics of small polyatomic molecules, photoionization, photodissociation and harmonic generation in strong laser fields, scattering of atoms/molecules from solid surfaces and propagation of light in optical devices by quantum-mechanical methods. He is an author of a text book, *Quantum Mechanics: A Chemistry Perspective* (Haifa, Israel: Technion Press—Michlol, 1996), and a co-author of over 170 journal articles.